GS2025-6

Investigation of volcanic rocks along the eastern margin of the sub-Phanerozoic Thompson nickel belt, central Manitoba (part of NTS 63J3) project update: preliminary lithogeochemistry and metamorphic petrology results

by C.G. Couëslan

In Brief:

- Arc basalt has been identified in the northern extension of the sub-Phanerozoic Winnipegosis komatiite belt, accompanied by evidence for local hydrothermal alteration
- Sedimentary rocks spatially associated with the volcanic rocks appear to be sourced from the Superior craton.
- The discovery of additional arc-volcanic rocks along strike from the Tower deposit could expand the area of VMS mineralization potential

Citation:
Couëslan, C.G. 2025: Investigation of volcanic rocks along the eastern margin of the sub-Phanerozoic Thompson nickel belt, central Manitoba (part of NTS 63J3) project update: preliminary lithogeochemistry and metamorphic petrology results; *in* Report of Activities 2025, Manitoba Business, Mining, Trade and Job Creation, Manitoba Geological Survey, p. 59–72.

Summary

An ongoing project to investigate metavolcanic rocks from the sub-Phanerozoic Superior boundary zone in Manitoba continued with geochemical and petrographic analyses of drillcore. The geochemistry of metasedimentary rocks suggests that they are likely sourced from the adjacent Superior craton; however, one sample of 'iron formation' from drillhole MRO-007 appears to be derived from basalt subjected to intense sericite alteration. Mafic rocks from the area can be subdivided into arc affinity and mid-ocean–ridge basalt affinity based on whole-rock geochemistry. The arc-affinity mafic rocks are restricted to an area previously mapped as Winnipegosis komatiite belt. Ultramafic volcanic rocks from drillhole NIM-068, within the Thompson nickel belt, are geochemically similar to aluminum undepleted komatiites.

Metapelite and metabasalt from the area mapped as Thompson nickel belt are characterized by middle amphibolite-facies metamorphic assemblages with a best estimate for pressure and temperature conditions of 3.25–3.5 kbar and 550–650 °C. Mafic rocks from the area mapped as Winnipegosis komatiite belt have mineral assemblages characteristic of the lower- to middle-amphibolite facies, and yield pressure and temperature estimates as low as 2.0–6.5 kbar and 460–540 °C. It is uncertain if a continuous metamorphic field gradient occurs between the Winnipegosis rocks and the rocks of the Thompson belt, or if a sharp, fault-bounded change in metamorphic grade exists.

The Tower deposit is the only known volcanogenic massive-sulphide deposit in the sub-Phanerozoic Superior boundary zone and is associated with arc-affinity volcanic rocks. The discovery of additional arc-affinity volcanic rocks along strike with the Tower deposit could indicate a greater potential for volcanogenic massive-sulphide–style mineralization in the area. The full tectonic significance of arc-affinity volcanics in the sub-Phanerozoic Superior boundary zone remains unknown.

Introduction

During the summer of 2024, a project was initiated in collaboration with HudBay Minerals Inc. to characterize metavolcanic rocks in the sub-Phanerozoic Superior boundary zone of Manitoba. Four drillholes, ranging from 16 to 28 km along strike from the Tower volcanogenic massive-sulphide (VMS) deposit (Figure GS2025-6-1), were selected for relogging to assess their affinities to Thompson nickel belt (TNB) rocks, Winnipegosis komatiite belt (WKB) rocks and the juvenile arc rocks that host the Tower deposit. Results from geochemical and petrographic analyses of the samples collected in 2024 are presented in this report. A more detailed description of the drillcore and the project can be found in Couëslan (2024). All rocks reported in this study were subjected to amphibolite-facies metamorphism; however, the 'meta-' prefix is not used for rock names in an effort to simplify the text.

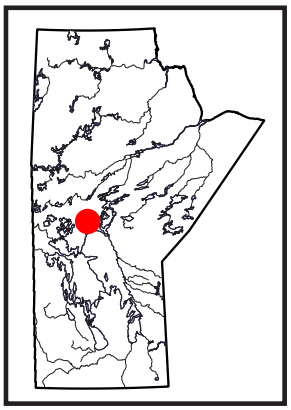

Geochemistry

Representative samples of each of the major rock types were collected for lithogeochemistry from each drillhole that was relogged in 2024. The data collected, and analytical methods used, can be found in Couëslan and Janssens (2025). The geochemistry of the sedimentary and volcanic rocks is discussed below.

Sedimentary rocks

Samples of sedimentary rocks were collected from drillholes MRO-005 and MRO-007 (Assessment File 73174, Manitoba Business, Mining, Trade and Job Creation, Winnipeg), which are interpreted from previous mapping to reside in the TNB and WKB, respectively (Figure GS2025-6-1). Multi-element profiles of pelitic rocks, normalized to the average P2 member pelite of the Ospwagan group

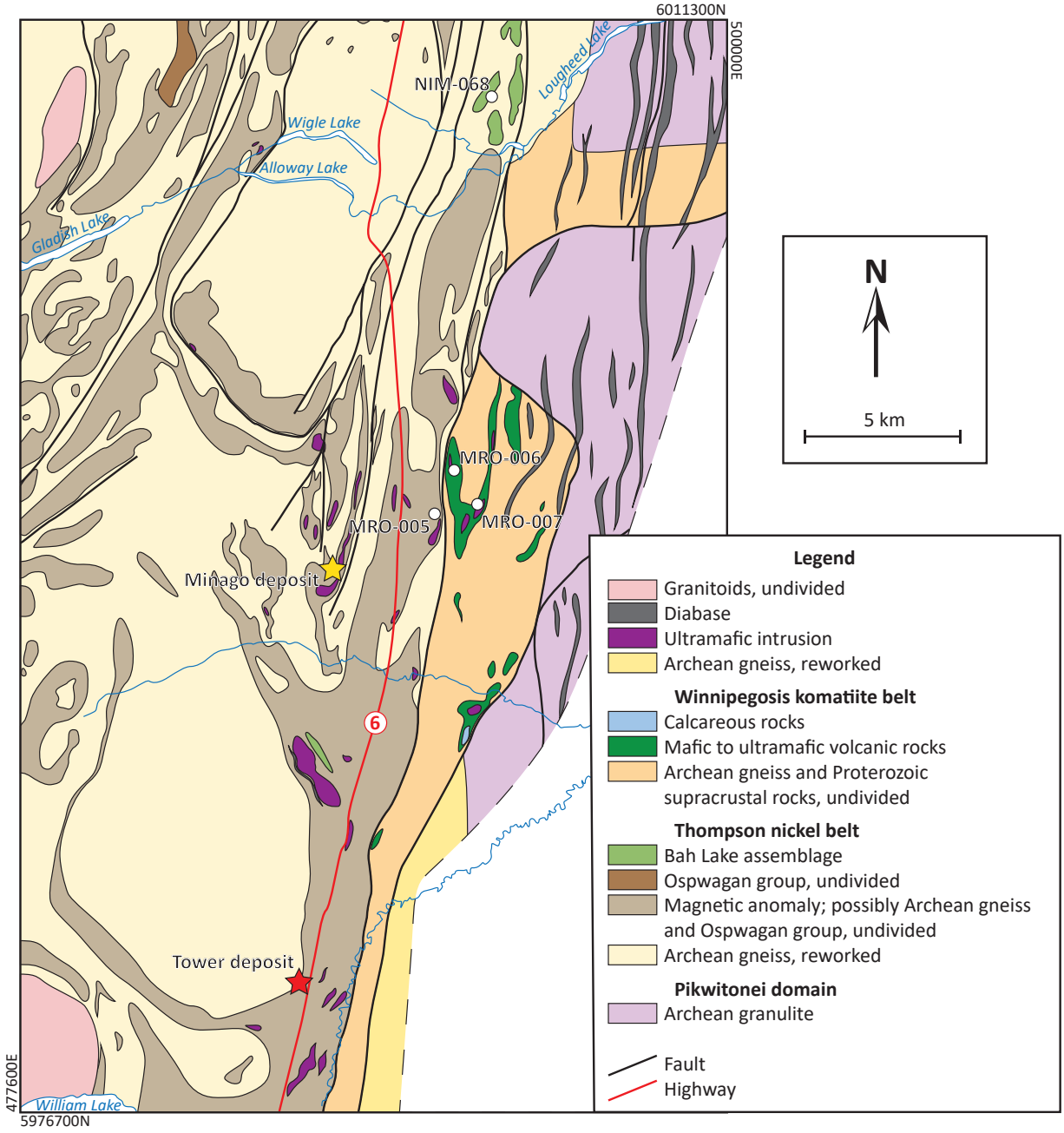

Figure GS2025-6-1: *Geology of the sub-Phanerozoic Superior boundary zone in the Minago River area (modified from Macek et al., 2006). Circles indicate the locations of drillholes from this study; the red star indicates a volcanogenic massive-sulphide deposit and the yellow star indicates a magmatic nickel deposit. All co-ordinates are in UTM Zone 14, NAD83.*

(Figure GS2025-6-2a; Zwanzig et al. 2007), are relatively flat and contrast with the weak positive slope typical of Burntwood group wacke from the Kisseynew domain (Figure GS2025-6-2b). The exception is the black shale from drillhole MRO-005, which is characterized by depletion at Al, Zr and Ti, and enrichment at V. In addition to V (526 ppm), the black shale is enriched in other redox-sensitive metals (280 ppm Ni, 170 ppm Cu, 660 ppm Zn, 46 ppm Mo).

A sample of 'impure chert' (108-24-011) from drillhole MRO-005 is enriched in iron (15.81 wt. % $Fe_2O_3^t$) and although it is characterized by quartz-rich laminations, the rock is not particularly siliceous (59.91 wt. % SiO_2). In addition to quartz, the rock is also biotite rich, which is reflected by a relatively high K_2O content (4.51 wt. %). The rock likely represents a combination of ferruginous, pelitic and siliceous sedimentary components. The normalized multi-element profile is relatively flat, with minor depletions at Th, Zr and Al (Figure GS2025-6-2c, d). The profile shares similarities with both iron formation from the P3 member and pelite from the P2 member of the Pipe formation. This is in strong contrast with the normalized profile of the magnetite-rich

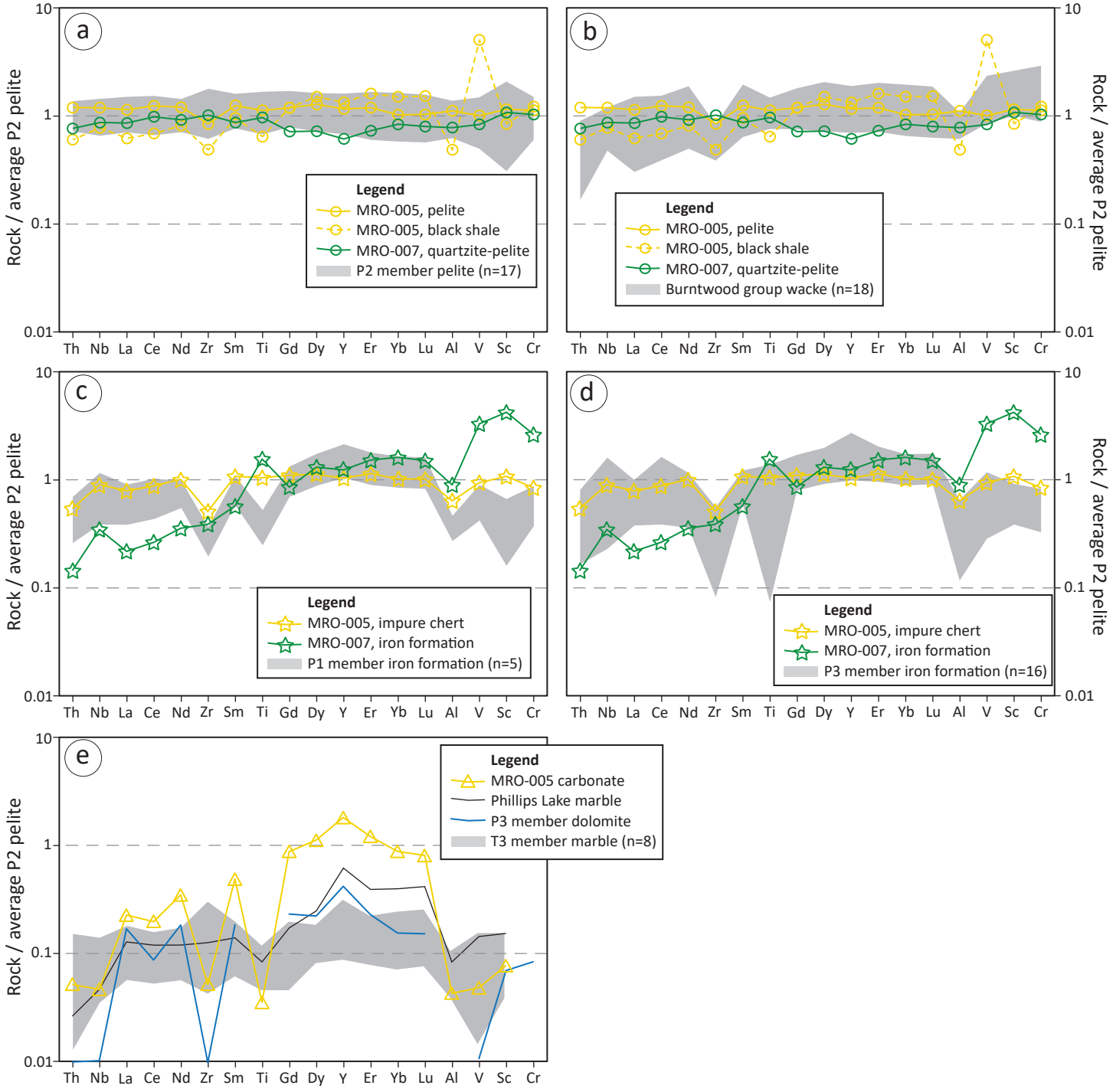

Figure GS2025-6-2: *Multi-element profiles of sedimentary rocks from the study area normalized to the average P2 pelite of Zwanzig et al. (2007) comparing:* ***a)*** *pelitic rocks with pelite from the P2 member of the Pipe formation;* ***b)*** *pelitic rocks with Burntwood group wacke;* ***c)*** *impure chert and iron formation with iron formation from the P1 member of the Pipe formation;* ***d)*** *impure chert and iron formation with iron formation from the P3 member of the Pipe formation;* ***e)*** *carbonate rock with marbles from Phillips Lake, the P3 member of the Pipe formation and the T3 member of the Thompson formation. Data sources: Burntwood group, Zwanzig et al. (2007); iron formations from the P1 and P3 members, Zwanzig et al. (2007) and Couëslan (2021); P2 member pelite, Zwanzig et al. (2007) and Couëslan (2022); P3 member dolomite, Zwanzig et al. (2007); T3 member marble, Zwanzig et al. (2007) and Couëslan (2016, 2021, 2022); Phillips Lake marble, Couëslan (2022).*

iron formation from drillhole MRO-007, which is characterized by a moderate positive slope and relative enrichments at Nb, Ti, V, Sc and Cr. The rock is characterized by abundant quartz-rich laminations and abundant magnetite (20.00 wt. %$Fe_2O_3^t$), which is typical of iron formations; however, it is also muscovite rich, with relatively abundant tourmaline (Figure GS2025-6-3a), and contains 15.87 wt. % Al_2O_3 and 5.91 wt. % K_2O, which is not typical of iron formations.

A second variety of impure chert (108-24-010) from drillhole MRO-005 consists of interlaminated chert and carbonate. This rock is characterized by a concave-down, normalized multi-element profile, with relative depletions at Nb, Zr, Ti, Al, V and Cr (Figure GS2025-6-2e). Although generally more enriched, the normalized profile does share a similar overall shape to that of other carbonate rocks from the TNB.

Mafic and ultramafic rocks

Basalt from drillholes MRO-005 and NIM-068 (Assessment Files 73174 and 73648; TNB; Figure GS2025-6-1) yields intermediate Mg# values (molar Mg/[Fe^T+Mg]; 0.44–0.54), which overlap the high-Fe tholeiite and high-Mg tholeiite fields of Jensen and Pyke (1982; Figure GS2025-6-4a). Chondrite-normalized rare-earth element (REE) profiles of the basalt are relatively flat to shallow sloping ($[La/Yb]_N$ = 0.90–1.79) and primitive mantle-normalized multi-element profiles are relatively flat to slightly concave down (Figure GS2025-6-5a–d). Drillhole NIM-068 also

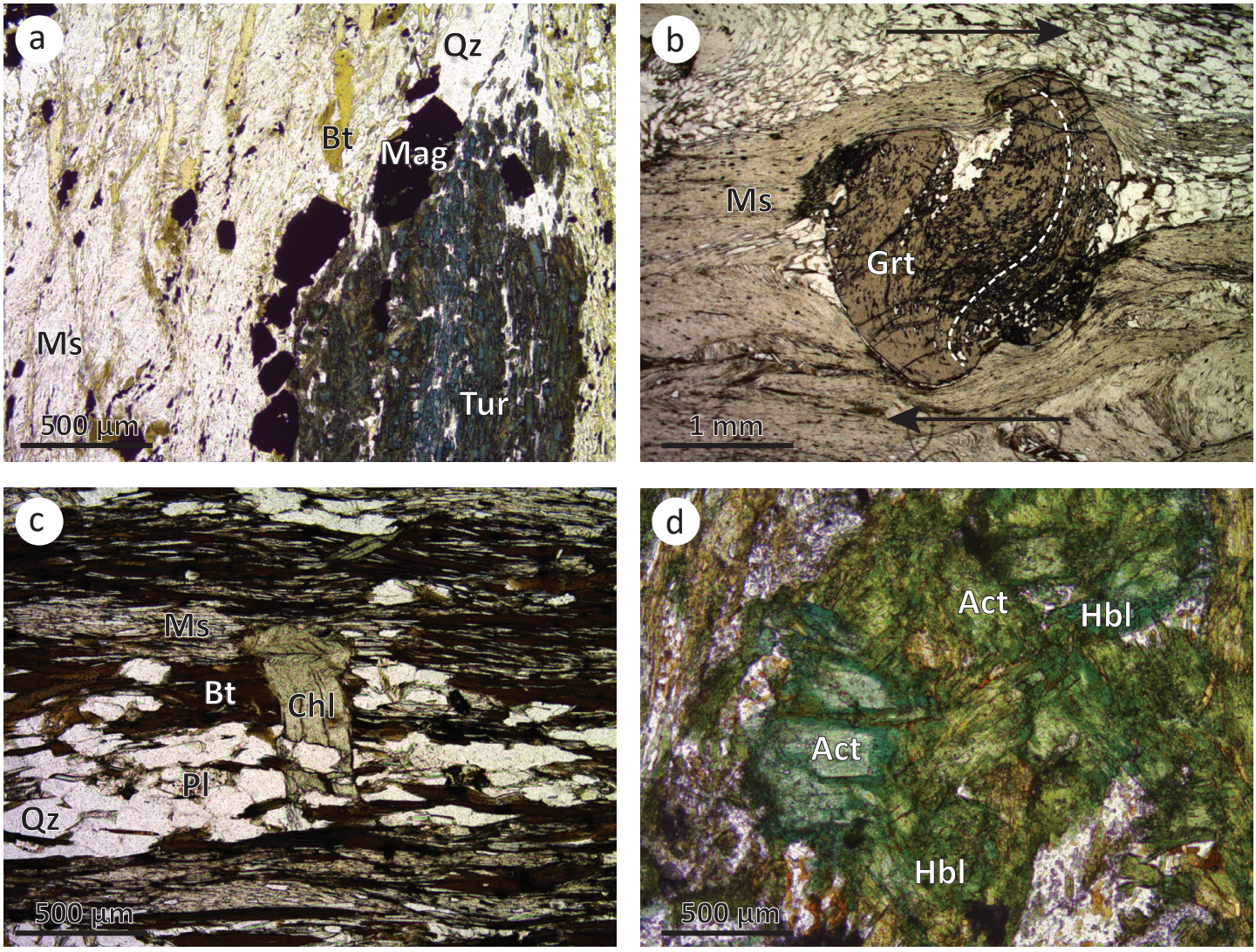

Figure GS2025-6-3: *Photomicrographs in plane-polarized light of samples from the study area:* ***a)*** *iron formation from drillhole MRO-007, with abundant muscovite, magnetite and tourmaline;* ***b)*** *rotated garnet porphyroblast in pelite from drillhole MRO-005, with inclusion-trail fabric in garnet indicated by dashed white line and direction of shear/rotation indicated by arrows;* ***c)*** *late chlorite crosscutting foliation in pelite from drillhole MRO-005, with foliation-parallel kink band present at the top of the chlorite grain;* ***d)*** *amphibole in gabbro from drillhole MRO-007, with pale actinolite cores and darker hornblende rims. Abbreviations: Act, actinolite; Bt, biotite; Chl, chlorite; Grt, garnet; Hbl, hornblende; Mag, magnetite; Ms, muscovite; Pl, plagioclase; Qz, quartz; Tur, tourmaline.*

contains ultramafic volcanic flows with Mg# values of 0.82–0.83, which plot within the komatiite field of Jensen and Pyke (1982; Figure GS2025-6-4a). The TiO_2 content of the ultramafic flows is 0.41–0.42 wt. %, and Al_2O_3/TiO_2 ratios of 15.5–19.5 and $(Gd/Yb)_N$ ratios of 0.91–1.32 are characteristic of aluminum undepleted komatiites (Nesbitt et al., 1979; Sproule et al., 2002). Normalized REE profiles of the ultramafic flows are relatively flat to concave down with negative Eu anomalies ($[La/Yb]_N$ = 1.03–1.14; Eu/Eu^* = 0.62–0.72; Figure GS2025-6-5c). Similarly, normalized multi-element profiles are relatively flat with pronounced positive anomalies at Th and negative anomalies at Nb (Figure GS2025-6-5d).

Three samples of basalt were collected from drillhole MRO-006 (Assessment Files 73174), including a sample with intense carbonate alteration, while one sample of basalt and one sample of gabbro were collected from MRO-007 (WKB; Figure GS2025-6-1). The unaltered basalt from MRO-006 plots within the high-Fe tholeiite field of Jensen and Pyke (1982; Figure GS2025-6-4a) and yields Mg# values of 0.41–0.43, whereas the gabbro and basalt from MRO-007 plot within the high-Mg tholeiite field and have Mg# values of 0.52–0.54.

Chondrite-normalized REE profiles of basalt from MRO-006 are characterized by moderate negative slopes for light REEs (LREEs) and flat to shallow negative slopes for medium and heavy REEs (MREEs and HREEs; $[La/Yb]_N$ = 2.28–2.71; Figure GS2025-6-5e). The carbonate altered basalt yields a similar normalized REE profile with a slight enrichment of LREEs ($[La/Yb]_N$ = 4.22). Primitive mantle-normalized multi-element profiles are characterized by negative slopes with negative anomalies at Nb (Figure GS2025-6-5f). The gabbro from MRO-007 yields normalized REE and multi-element profiles that are similar to the basalt from MRO-006, but with a slightly more pronounced negative slope to the MREEs ($[La/Yb]_N$ = 3.92; Figure GS2025-6-5g, h). In contrast, the basalt from MRO-007 yields a relative flat normalized REE profile ($[La/Yb]_N$ = 0.95) and slightly concave-down normalized multi-element profile (Figure GS2025-6-5g, h).

Discussion of geochemistry

The majority of sedimentary rocks yield normalized multi-element profiles similar to Ospwagan group rocks of the TNB (Figure GS2025-6-2). The similarity in profiles is indicative of a similar detrital source, which in this case is likely the Superior craton; however, it may be premature to assume a direct correlation with the Ospwagan group. As discussed in Couëslan (2024), none of the sequences described from the drillcore make for straightforward correlations with Ospwagan group stratigraphy.

Although the normalized profile of the black shale from MRO-005 bares some similarity to Burntwood group rocks of the Kisseynew domain, the Burntwood group typically occurs as a monotonous succession of turbidite deposits. Volcanogenic rocks, chert and carbonate rocks are rare. In contrast, the black shale occurs as deposits between basalt flows, along with interlaminated chert and carbonate rocks. In addition, the abundance of sulphide and graphite, and negative anomalies at Al, Ti and Zr indicate detritus-starved deposits, which were likely influenced by strongly reducing conditions, as suggested by enrichment in redox-sensitive metals. Chemistry of the black shale could also have been influenced by small amounts of basalt-derived detritus.

The normalized profile of the iron formation from MRO-007 is in strong contrast to the profiles of similar Ospwagan group rocks. The positive slope of the iron formation's profile, along with positive anomalies at Nb, Ti, V and Sc, is indicative of a mafic igneous rock (Figure GS2025-6-2c, d; cf. Couëslan, 2018). The modified Zr/TiO_2-Ni diagram of Couëslan (2018) effectively subdivides the mafic igneous rocks from the sedimentary rocks (Figure GS2025-6-4b). Although it is more enriched in Ni, the iron formation from MRO-007 has a similar Zr/TiO_2 value as the basalts, and would lie close to the projected dividing line between the igneous rock field and the sedimentary rock field. In addition, it plots well outside the field defined by Ospwagan group iron formations. The iron formation also plots tightly clustered with the mafic rocks in the basalt field of the Zr/Ti-Nb/Y diagram of Pearce (1996; Figure GS2025-6-4c), and is distinct from Ospwagan group iron formations and the impure chert from MRO-005. Finally, chondrite- and primitive mantle-normalized profiles of the iron formation from MRO-007 are similar to the profiles of the gabbro from MRO-007 and basalt from MRO-006 (Figure GS2025-6-6a, b).

The atypical mineral assemblage for the iron formation (dominantly quartz+magnetite+muscovite), combined with the geochemical evidence, suggests that it represents a mafic igneous rock that was hydrothermally altered prior to peak metamorphism. Alteration indices were calculated for the iron formation, as well as the mafic and ultramafic igneous rocks of this study, using the NORMAT approach of Piché and Jébrak (2004; Table GS2025-6-1). The technique uses a normative mineral approach to calculate the overall intensity of alteration (IFRAIS), as well as specific normative mineral alteration indices for paragonite (IPARA), sericite (ISER), chlorite (ICHLO), pyrophyllite (IPYRO) and carbonatization (IPAF). The carbonatization index is calculated by comparing the measured loss-on-ignition (LOI) values with the normative LOI values. Because the rocks contain amphibolite-facies mineral assemblages (see Metamorphic petrology section) and the normative calculations are for greenschist-facies assemblages, the IPAF values are likely an underestimate. All samples of mafic and ultramafic rocks yield IFRAIS values of 100, indicating relatively fresh and unaltered protolith. Only the carbonate-altered basalt sample from MRO-006 yielded an IPAF value of 4.50, indicating minor carbonatization. The iron formation from MRO-007 yielded an IFRAIS value of 28.6, indicating intense hydrothermal alteration of the protolith. The alteration is calculated to be dominantly sericite (ISER = 65.7), with minor paragonite (IPARA = 5.74).

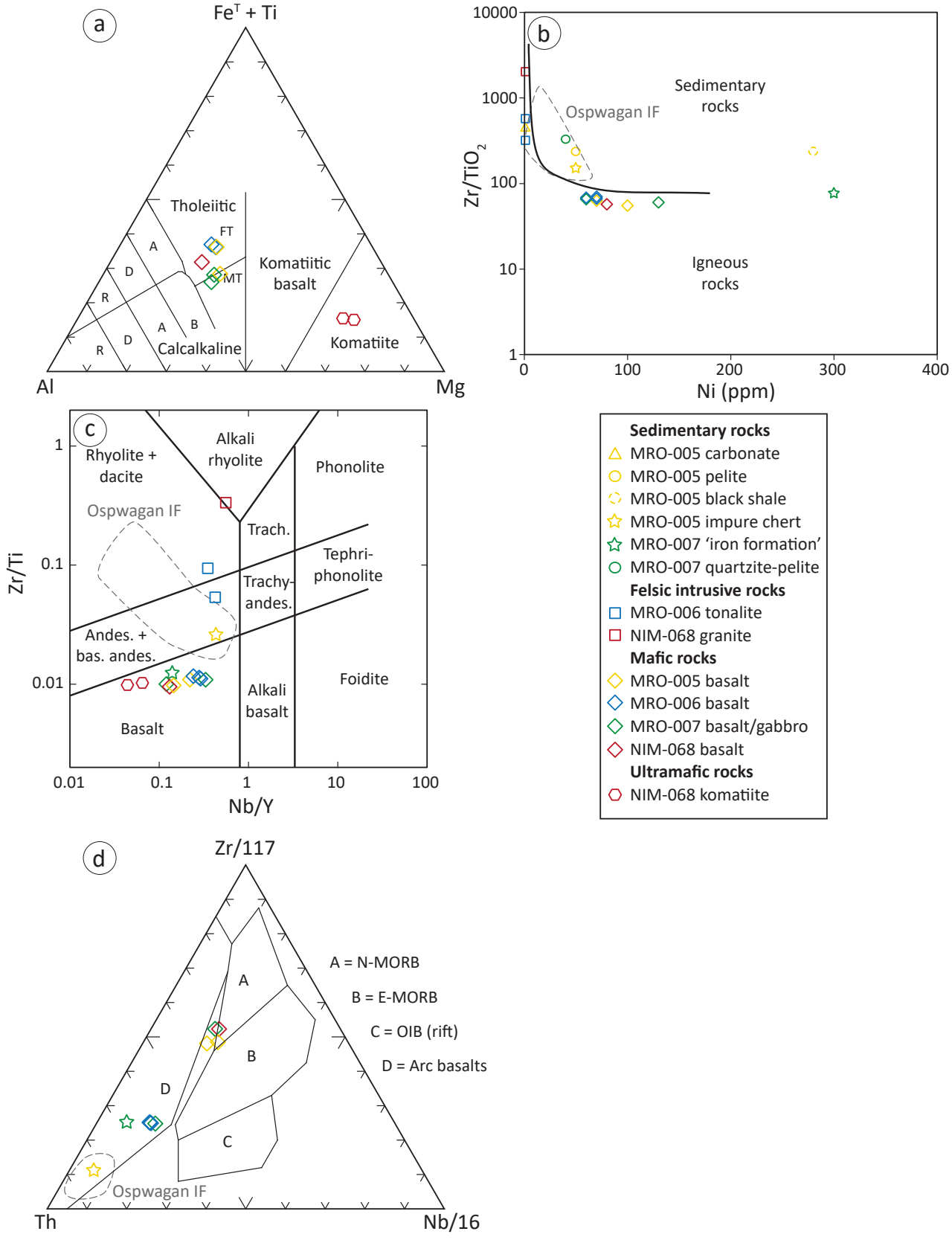

Figure GS2025-6-4: *Geochemical discrimination diagrams of samples from the study area:* ***a)*** *Al–Fe+Ti–Mg diagram (after Jensen and Pyke, 1982);* ***b)*** *Ni–Zr/TiO$_2$ diagram (after Couëslan, 2018; adapted from Winchester et al., 1980);* ***c)*** *Nb/Y–Zr/Ti diagram (after Pearce, 1996);* ***d)*** *Th–Zr–Nb diagram (after Wood et al., 1979). Abbreviations: A, andesite; Andes., andesite; B, basalt; bas., basaltic; D, dacite; E-MORB, enriched mid-ocean–ridge basalt; FT, high-Fe tholeiite; IF, iron formation; MT, high-Mg tholeiite; N-MORB, normal mid-ocean–ridge basalt; OIB, oceanic-island basalt; R, rhyolite; Trach., trachyte. Reference data for Ospwagan group iron formation from Zwanzig et al. (2007) and Couëslan (2021).*

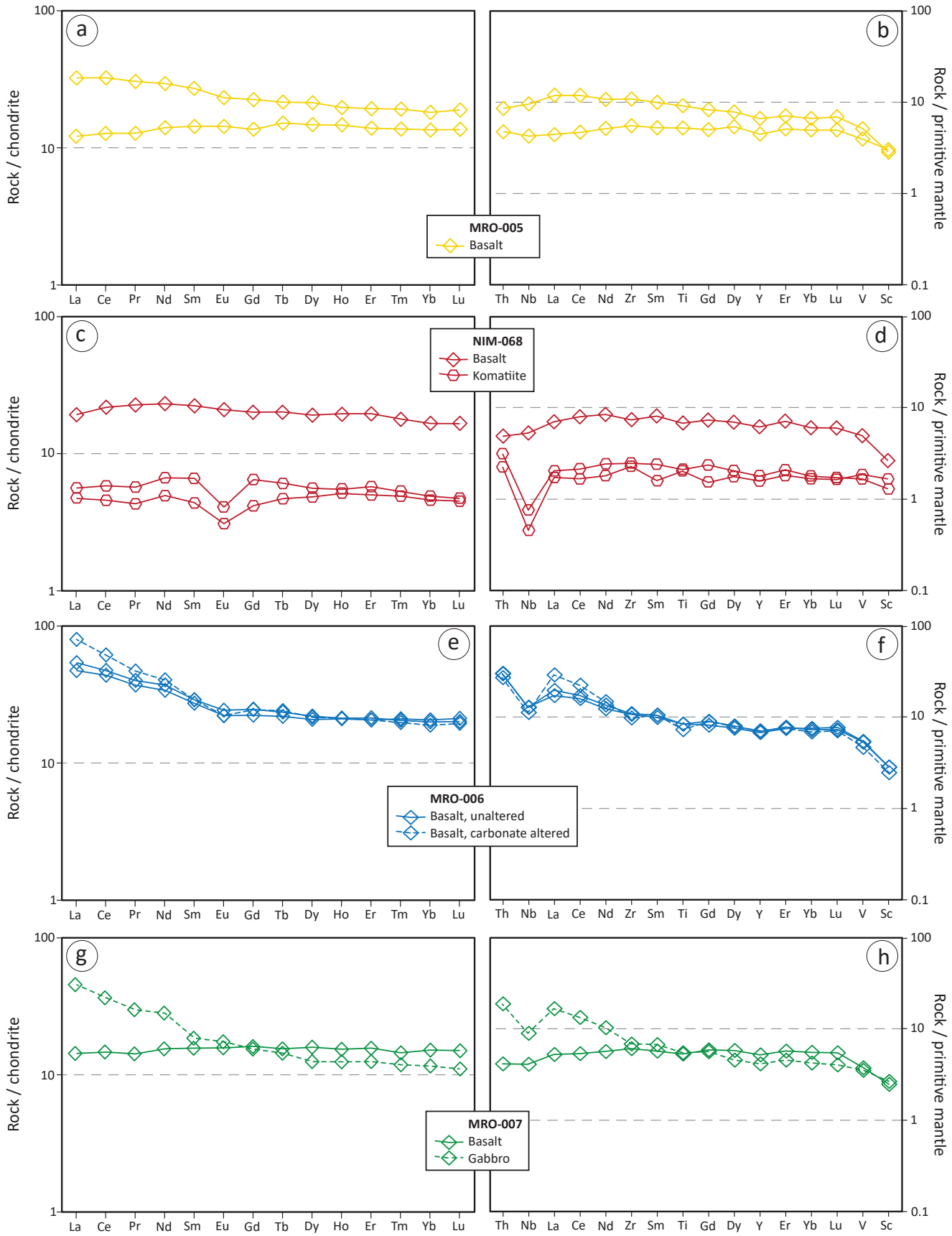

Figure GS2025-6-5: *Chondrite-normalized rare-earth element profiles (left column) and primitive mantle-normalized multi-element profiles (right column) of mafic and ultramafic rocks from the study area:* ***a), b)*** *basalt from drillhole MRO-005;* ***c), d)*** *basalt and komatiite from drillhole NIM-068;* ***e), f)*** *unaltered and altered basalt from drillhole MRO-006;* ***g), h)*** *basalt and gabbro from drillhole MRO-007. Normalizing values for chondrite and primitive mantle are from McDonough and Sun (1995).*

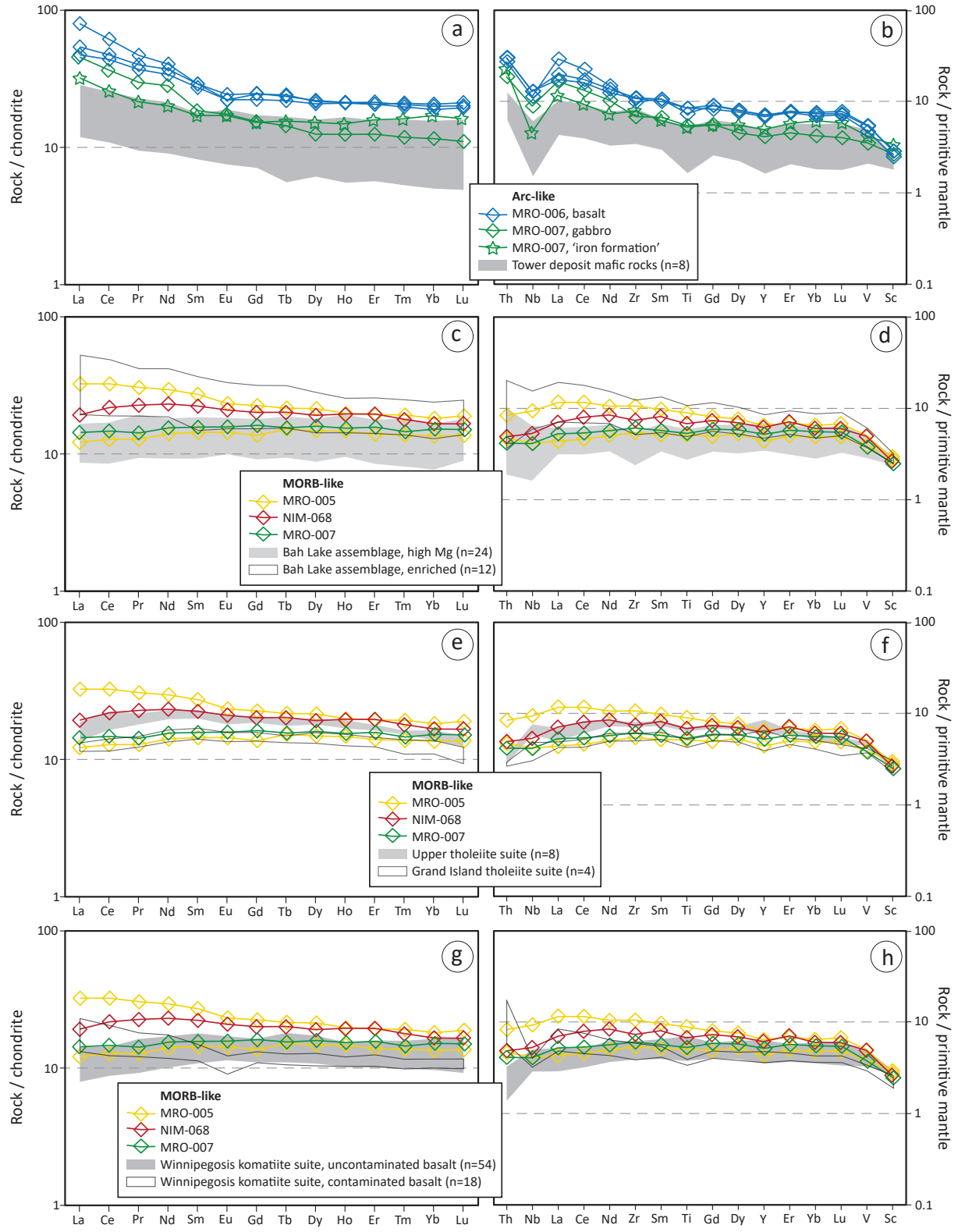

Figure GS2025-6-6: *Chondrite-normalized rare-earth element profiles (left column) and primitive mantle-normalized multi-element profiles (right column) of mafic rocks from the study area compared with other mafic rocks from the Thompson nickel belt and Winnipegosis komatiite belt:* ***a), b)*** *arc-affinity rocks from drillholes MRO-006 and MRO-007 compared with Tower deposit mafic rocks;* ***c), d)*** *MORB-affinity rocks from drillholes MRO-005, MRO-007 and NIM-068 compared with Bah Lake assemblage rocks;* ***e), f)*** *MORB-affinity rocks from drillholes MRO-005, MRO-007 and NIM-068 compared with the Upper tholeiite suite and the Grand Island tholeiite suite;* ***g), h)*** *MORB-affinity rocks from drillholes MRO-005, MRO-007 and NIM-068 compared with basalts from the Winnipegosis komatiite suite. Normalizing values for chondrite and primitive mantle are from McDonough and Sun (1995). Data sources: Bah Lake assemblage, Zwanzig (2005); Grand Island tholeiite suite, Burnham et al. (2009); Tower deposit mafic rocks, Couëslan (2018); Upper tholeiite suite, Burnham et al. (2009); Winnipegosis komatiite suite uncontaminated basalt, Ciborowski et al. (2017) and Waterton et al. (2017); Winnipegosis komatiite suite contaminated basalt, Burnham et al. (2009).*

The mafic igneous rocks in this study can be subdivided into two geochemical groups: one with relatively flat normalized REE and multi-element profiles ($[La/Yb]_N$ <1.8) suggestive of mid-ocean–ridge basalt (MORB)-affinity rocks; and the other with negative-sloping REE and multi-element profiles ($[La/Yb]_N$ >1.8), and prominent negative Nb anomalies suggestive of arc-affinity rocks. This subdivision is readily apparent on the Th-Zr-Nb diagram of Wood et al. (1979; Figure GS2025-6-4d). Several suites of MORB-affinity basalt occur in the region, including the Bah Lake volcanic assemblage of the TNB, and the Upper tholeiite suite, Grand Island suite and Winnipegosis suite of the WKB (Figure GS2025-6-6c–h). In contrast, arc-affinity basalt is only known from the sequence that hosts the Tower VMS deposit (Couëslan, 2018; Figure GS2025-6-6a, b).

Metamorphic petrology

Pelites

The two most commonly used bulk compositions for metamorphic studies are pelitic rocks and mafic rocks. Whereas mafic rocks are found in all of the examined drillcore, pelitic rocks are found only in holes MRO-005 and MRO-007 (Figure GS2025-6-1). The pelite from MRO-007 contains abundant muscovite and quartz, along with subordinate biotite, epidote, titanite and pyrite, and accessory carbonate and tourmaline. This mineral assemblage is not particularly informative for estimating metamorphic grade; however, the absence of chlorite and abundance of muscovite suggest peak metamorphic conditions of lower- to middle-amphibolite facies.

The pelite from drillhole MRO-005 contains the assemblage quartz-muscovite-biotite-garnet-staurolite-chlorite-plagioclase-ilmenite. Muscovite and biotite define a well-developed foliation, in which rare biotite 'fish' are wrapped by the fabric. Garnet and staurolite form poikiloblasts with inclusion trails indicating rotation and syntectonic growth (Figure GS2025-6-3b). Chlorite typically occurs as replacement of biotite and staurolite and locally crosscuts the foliation suggesting it is a relatively late, retrograde metamorphic mineral (Figure GS2025-6-3c). Local kink bands within the chlorite grains have boundaries parallel to the foliation, which suggests that deformation outlasted chlorite growth. The plagioclase occurs as relatively sparse grains that are intensely altered to sericite. The peak metamorphic assemblage of quartz-muscovite-biotite-garnet-staurolite-plagioclase-ilmenite is diagnostic of the middle-amphibolite facies in pelitic rocks.

Mafic rocks

Basalt samples from drillhole MRO-005 contain hornblende–plagioclase–quartz–Fe-Ti oxide–Fe sulphide±biotite ±cummingtonite. Where present, cummingtonite occurs as acicular to xenomorphic overgrowths on hornblende. Larger

Table GS2025-6-1: Normative mineral alteration indices calculated for mafic and ultramafic rocks from the study area using the NORMAT method of Piché and Jébrak (2004).

Sample	Rock type	IFRAIS[1]	IPARA[2]	ISER[3]	ICHLO[4]	IPYRO[5]	IPAF[6]
108-24-002	Metabasalt	100.00	0.00	0.00	0.00	0.00	N/A
108-24-005	Metabasalt	100.00	0.00	0.00	0.00	0.00	N/A
108-24-006	Metabasalt, carbonate-altered	100.00	0.00	0.00	0.00	0.00	4.50
108-24-008	Metabasalt	100.00	0.00	0.00	0.00	0.00	N/A
108-24-012	Metabasalt	100.00	0.00	0.00	0.00	0.00	N/A
108-24-013	Metabasalt	100.00	0.00	0.00	0.00	0.00	N/A
108-24-018	Metagabbro	100.00	0.00	0.00	0.00	0.00	N/A
108-24-019	Metabasalt	100.00	0.00	0.00	0.00	0.00	N/A
108-24-014	Komatiite	100.00	0.00	0.00	0.00	0.00	N/A
108-24-015	Komatiite	100.00	0.00	0.00	0.00	0.00	N/A
108-24-020	Iron formation	28.60	5.74	65.66	0.00	0.00	N/A

[1] Index of alkali-element depletion; lower numbers indicate an increase in the intensity of the depletion

[2] Index of paragonitization; higher numbers indicate increasing intensity

[3] Index of sericitization; higher numbers indicate increasing intensity

[4] Index of chloritization; higher numbers indicate increasing intensity

[5] Index of pyrophyllitization; higher numbers indicate increasing intensity

[6] Index of carbonatization; higher numbers indicate increasing intensity; samples with measured LOI <normative LOI = N/A

Abbreviations: LOI, loss-on-ignition; N/A, not applicable

hornblende grains contain rare cores of actinolite, which are interpreted as a relict, prograde metamorphic phase. Plagioclase occurs along with quartz as aggregates of xenomorphic grains. Local twinning indicates compositions near the oligoclase–andesine boundary as determined optically using a universal stage. The prograde assemblage of hornblende-plagioclase-quartz±cummingtonite±biotite is indicative of the amphibolite-facies for mafic rocks.

A single basalt sample was collected from drillhole NIM-068, which contains the mineral assemblage hornblende–plagioclase–quartz–titanite–Fe-Ti oxide–Fe sulphide. The plagioclase and quartz form a fine- to medium-grained, granoblastic groundmass. Optical determinations of abundant twining indicate a plagioclase composition of andesine. Titanite occurs as aggregates of xenomorphic grains along discontinuous laminations. The observed assemblage is characteristic of the amphibolite facies.

Basalt samples from drillhole MRO-006 contain hornblende–plagioclase–biotite–epidote–quartz–Fe-Ti oxide–Fe-sulphide±calcite. Larger hornblende grains contain rare cores of actinolite, which are interpreted as a relict, prograde metamorphic phase. The plagioclase is untwinned and typically intergrown with quartz in flattened aggregates/lenses. When present, the calcite is typically associated with the plagioclase-quartz lenses. The mineral assemblage hornblende-plagioclase-epidote-quartz±biotite is indicative of the lower- to middle-amphibolite facies for metabasites.

A gabbro sample from drillhole MRO-007 contains the assemblage actinolite–hornblende–plagioclase–epidote–quartz–biotite–titanite–Fe-Ti oxide. The hornblende typically occurs as overgrowths on, and along fractures within, the actinolite (Figure GS2025-6-3d). Plagioclase is untwinned and intergrown with quartz. The plagioclase-quartz segregations are commonly intergrown with epidote, biotite and acicular hornblende. The titanite typically occurs as polycrystalline aggregates enclosing Fe-Ti oxide. The mineral assemblage actinolite-hornblende-plagioclase-epidote-quartz is typical of lower-amphibolite–facies conditions near the greenschist-facies transition. A basalt sample from the same drillhole contains the assemblage hornblende–plagioclase–quartz–epidote–Fe-Ti oxide–Fe sulphide. Larger hornblende grains contain rare cores of actinolite, which is interpreted as a relict phase. Plagioclase is untwinned and is intergrown with quartz as polycrystalline aggregates. The aggregates contain sparse epidote and acicular hornblende. The metamorphic assemblage is typical of the lower- to middle-amphibolite facies for metabasites.

Phase-equilibria modelling and discussion of metamorphism

Phase-equilibria diagrams were calculated for select mafic rocks from each of the drillholes and pelite from dillhole MRO-005. The diagrams were calculated using the Theriak–Domino software package (de Capitani and Petrekakis, 2010) and the updated 2003 ds5.5 thermodynamic dataset of Holland and Powell (1998), and used activity models outlined in Tinkham and Ghent (2005), Pattison and Tinkham (2009), and Couëslan et al. (2011). The pelite was calculated in the system MnO-Na_2O-CaO-K_2O-FeO-MgO-Al2O_3-SiO2-H_2O-TiO_2 (MnNCKFMASHT), whereas the mafic rocks were calculated in the systems Na_2O-CaO-K_2O-FeO-MgO-Al_2O_3-SiO_2-H_2O-TiO_2-Fe_2O_3 (NCKFMASHTO), or NCF-MASHTO if whole-rock K_2O <0.5 wt. %. An Fe_2O_3/FeO ratio of 0.20 was used for all mafic rocks following Middlemost (1989).

The pelite sample from drillhole MRO-005 (108-24-007) contains the peak metamorphic assemblage quartz-muscovite-biotite-garnet-staurolite-plagioclase-ilmenite. The observed assemblage defines an area in modelled pressure-temperature (P-T) space of roughly 3.25–5.5 kbar and 550–650 °C (Figure GS2025-6-7a). The mineral assemblage observed in a basalt sample from the same drillhole (108-24-012) contains hornblende–plagioclase–quartz–Fe-Ti oxide. Actinolite is present as rare cores within larger hornblende grains but is interpreted as a relict, prograde phase. The observed peak metamorphic assemblage defines an area in the modelled P–T space of >3.75 kbar and >550 °C (Figure GS2025-6-7b). Although the observed assemblage from the basalt provides a poor constraint on the peak metamorphic pressure and temperature, it does overlap with the P-T conditions calculated for the peak assemblage in the pelite, which suggests agreement between the models.

A basalt sample (108-24-013) from drillhole NIM-068 contains a peak metamorphic assemblage of hornblende–plagioclase–quartz–titanite–Fe-Ti oxide. The observed assemblage defines a rather large field in modelled P-T space of roughly 2.0–6.8 kbar and 480–640 °C (Figure GS2025-6-7c).

Basalt sample 108-24-002 from drillhole MRO-006 contains a peak metamorphic assemblage of hornblende–biotite–plagioclase–quartz–epidote–Fe-Ti oxide. The observed assemblage is not predicted to occur in the modelled system without the presence of titanite. It is possible that trace amounts of titanite could be present in the rock and either were not identified or misidentified as epidote. Alternatively, titanite could be an artifact generated by the activity models used to calculate the phase equilibria. The observed assemblage plus titanite defines a relatively narrow field that covers a large part of the modeled P–T space from roughly 2–8 kbar and 480–650 °C (Figure GS2025-6-8a).

A metagabbro sample (108-24-018) from drillhole MRO-007 contains the mineral assemblage actinolite–hornblende–plagioclase–epidote–quartz–biotite–titanite–Fe-Ti oxide. No field with the observed assemblage is predicted in the modelled P–T space; however, the observed assemblage, minus Fe-Ti oxide, defines a field with relatively poor pressure constraints (roughly 2.0–6.5 kbar) but good temperature constraints (460–540 °C; Figure GS2025-6-8b). The presence of titanite as rims on Fe-Ti oxides in thin section indicates that titanite is a stable Ti-bearing phase in the assemblage. A small field with stable magnetite is present at approximately 2 kbar and 450 °C. It is possible that

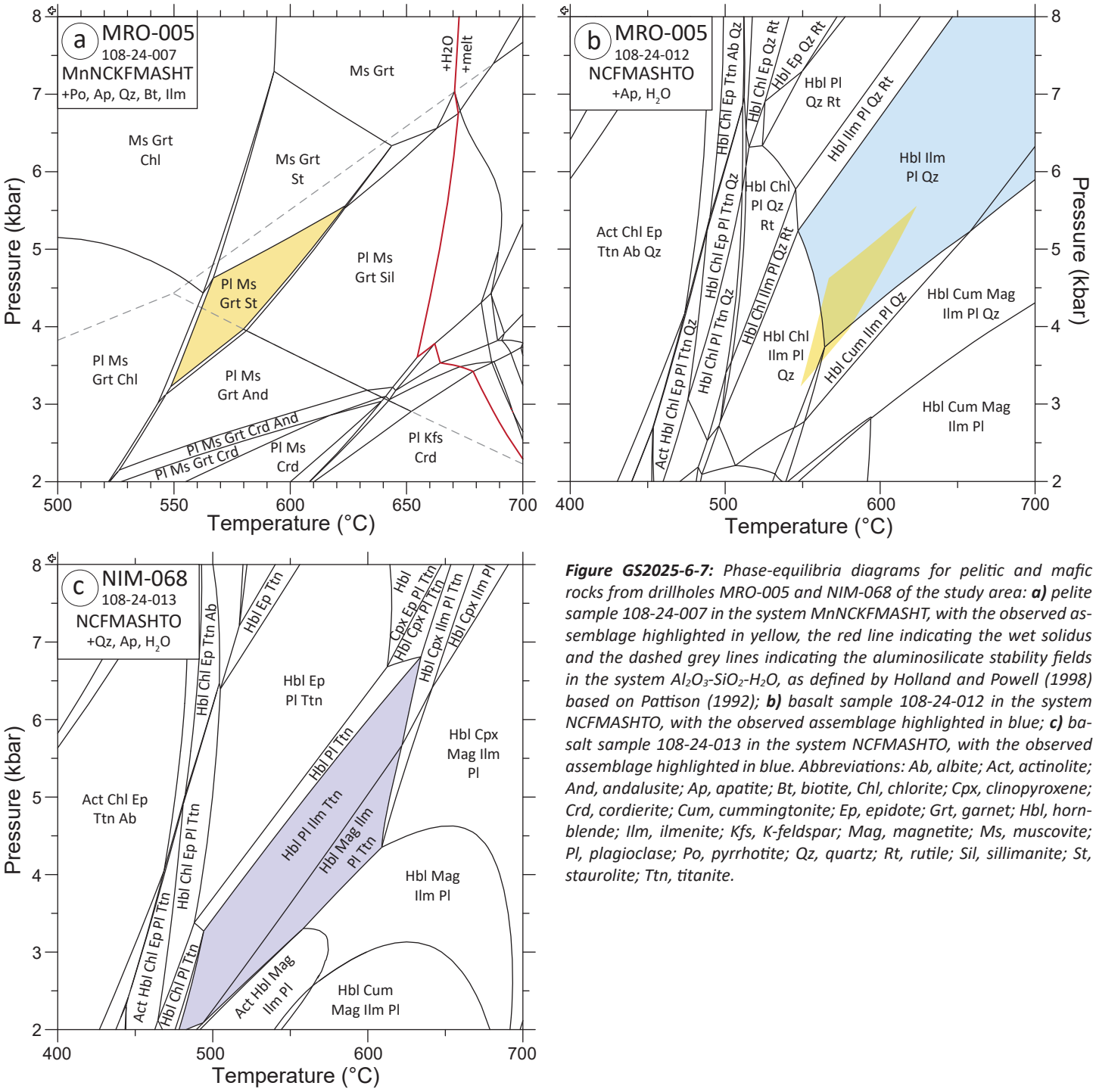

Figure GS2025-6-7: *Phase-equilibria diagrams for pelitic and mafic rocks from drillholes MRO-005 and NIM-068 of the study area:* ***a)*** *pelite sample 108-24-007 in the system MnNCKFMASHT, with the observed assemblage highlighted in yellow, the red line indicating the wet solidus and the dashed grey lines indicating the aluminosilicate stability fields in the system Al_2O_3-SiO_2-H_2O, as defined by Holland and Powell (1998) based on Pattison (1992);* ***b)*** *basalt sample 108-24-012 in the system NCFMASHTO, with the observed assemblage highlighted in blue;* ***c)*** *basalt sample 108-24-013 in the system NCFMASHTO, with the observed assemblage highlighted in blue. Abbreviations: Ab, albite; Act, actinolite; And, andalusite; Ap, apatite; Bt, biotite, Chl, chlorite; Cpx, clinopyroxene; Crd, cordierite; Cum, cummingtonite; Ep, epidote; Grt, garnet; Hbl, hornblende; Ilm, ilmenite; Kfs, K-feldspar; Mag, magnetite; Ms, muscovite; Pl, plagioclase; Po, pyrrhotite; Qz, quartz; Rt, rutile; Sil, sillimanite; St, staurolite; Ttn, titanite.*

relict magnetite from along the prograde path of metamorphism forms the oxide core to the titanite rims.

In general, rocks from the areas mapped as TNB appear to be metamorphosed to a slightly higher metamorphic grade than rocks from the WKB. The TNB rocks contain mineral assemblages typical of the middle-amphibolite facies, with the best peak P-T constraints provided by the pelite from hole MRO-005 at 3.25–5.5 kbar and 550–650 °C (Figure GS2025-6-7a). The WKB rocks contain epidote±actinolite-bearing mineral assemblages typical of the lower- to middle-amphibolite facies. Assuming that there is no metamorphic field gradient between drillholes MRO-006 and MRO-007, the metamorphic grade for these rocks could be further constrained by overlaying the observed mineral assemblages from samples 108-24-002 and 108-24-018 in P-T space (Figure GS2025-6-8c). The overlap between the fields defined by the observed assemblages indicate P-T conditions of roughly 2.5–4.5 kbar and 480–540 °C. In this scenario, a relatively sharp change in metamorphic grade could occur between the TNB rocks and the WKB rocks, possibly along a fault structure. However, it is equally possible that a continuous westward increase

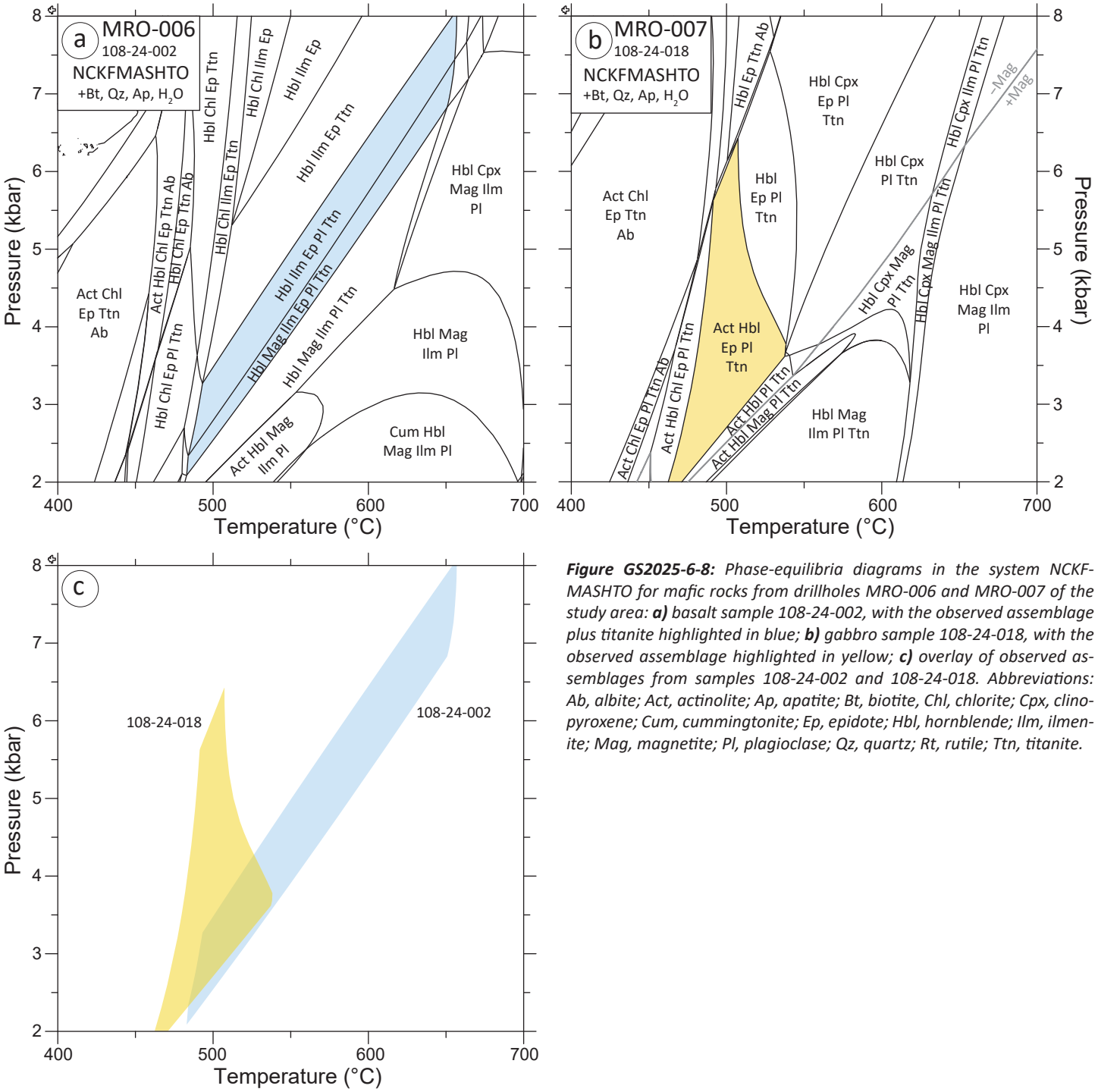

Figure GS2025-6-8: *Phase-equilibria diagrams in the system NCKFMASHTO for mafic rocks from drillholes MRO-006 and MRO-007 of the study area:* ***a)*** *basalt sample 108-24-002, with the observed assemblage plus titanite highlighted in blue;* ***b)*** *gabbro sample 108-24-018, with the observed assemblage highlighted in yellow;* ***c)*** *overlay of observed assemblages from samples 108-24-002 and 108-24-018. Abbreviations: Ab, albite; Act, actinolite; Ap, apatite; Bt, biotite, Chl, chlorite; Cpx, clinopyroxene; Cum, cummingtonite; Ep, epidote; Hbl, hornblende; Ilm, ilmenite; Mag, magnetite; Pl, plagioclase; Qz, quartz; Rt, rutile; Ttn, titanite.*

in metamorphic grade occurs from drillhole MRO-007 in the WKB (with the lowest P-T estimates and actinolite-hornblende-epidote–bearing assemblages), toward drillhole MRO-005 in the TNB (with notably higher P-T estimates, and actinolite- and epidote-free assemblages; Figure GS2025-6-1). This scenario would be similar to the exposed portions of the TNB, where metamorphic field gradients are steepest perpendicular to the strike of the belt (Couëslan and Pattison, 2012). Further refinement of the models may provide insight into this problem.

Economic considerations

Volcanogenic massive-sulphide deposits are an important mineral deposit type in the juvenile terranes of the Trans-Hudson orogen of Manitoba, where they are associated with arc-affinity volcanic rocks (Bailes and Galley, 1999; Syme et al., 1999; Tucker et al., 2005; Simard et al., 2010). The only known VMS deposit in the Superior boundary zone of Manitoba is the Tower deposit (Couëslan, 2018), which is also associated with juvenile arc-affinity volcanic rocks. Economic VMS deposits rarely occur

in isolation as demonstrated by the Flin Flon and Snow Lake mining camps. The identification of additional arc-affinity rocks approximately 15 km along strike of the Tower deposit suggests a larger area with potential to host VMS deposits than previously recognized. Intense sericitic alteration of basalt in drillhole MRO-007 suggests the potential development of at least localized, synvolcanic hydrothermal systems. Immediately above this zone of hydrothermal alteration is a siliceous rock with pyrite laminations that was previously interpreted as a quartzite (Couëslan, 2024). This unit should be revisited to see if it could be derived from felsic volcanic rocks.

The presence of arc-affinity volcanic rocks in what was previously mapped as the WKB raises many questions regarding current understanding of the Precambrian geology in this part of the province and the potential for VMS exploration. The arc rocks of the Tower deposit were interpreted as a klippe or erosional remnant of juvenile arc rocks that were thrust onto the Superior margin during the Trans-Hudson orogeny (Couëslan, 2018). Could the arc rocks in drillholes MRO-006 and MRO-007 be part of the same, or a similar, structure? Is the klippe model still valid, or could a belt of juvenile arc rocks have formed along the Superior margin? The WKB is interpreted to have formed in an evolving rift environment (Ciborowski et al., 2017; Waterton et al., 2017). Could rifting have progressed until the development of a juvenile arc was possible during closure of the rift basin? In this scenario, why would the arc rocks be preserved at the northern terminus of the belt rather than farther south, where the WKB (and presumably the rift basin) was substantially thicker? It is hoped that samples submitted for isotope geochemistry might help answer some of these questions; however, they may remain largely unanswered without additional information from drillcore.

Acknowledgments

The author thanks N. Richardson and C. Venturi from HudBay Minerals Inc. for their continued support of this project. Thanks to T. Martins, J. Macdonald and K. Reid for reviewing earlier drafts of the report.

References

Bailes, A.H. and Galley, A.G. 1999: Evolution of the Paleoproterozoic Snow Lake arc assemblage and geodynamic setting for associated volcanic-hosted massive sulphide deposits, Flin Flon Belt, Manitoba, Canada; Canadian Journal of Earth Sciences, v. 36, p. 1789–1805.

Burnham, O.M., Halden, N., Layton-Matthews, D., Lesher, C.M., Liwanag, J., Heaman, L., Hulbert, L., Machado, N., Michalak, D., Pacey, M., Peck, D.C., Potrel, A., Theyer, P., Toope, K. and Zwanzig, H. 2009: CAMIRO project 97E-02, Thompson Nickel Belt: final report, March 2002, revised and updated 2003; Manitoba Science, Technology, Energy and Mines, Manitoba Geological Survey, Open File OF2008-11, 434 p., plus appendices and GIS shape files for use with ArcInfo®.

Ciborowski, T.J.R., Minifie, M.J., Kerr, A.C., Ernst, R.E., Baragar, B. and Millar, I.L. 2017: A mantle plume origin for the Paleoproterozoic circum-Superior large igneous province; Precambrian Research, v. 294, p. 189–213.

Couëslan, C.G. 2016: Whole-rock lithogeochemistry, Sm-Nd isotope geochemistry, and U-Pb zircon geochronology for samples from the Paint and Phillips lakes area, Manitoba (parts of NTS 63O1, 8, 9, 63P5, 12); Manitoba Growth Enterprise and Trade, Manitoba Geological Survey, Data Repository Item DRI2016001, Microsoft® Excel® file.

Couëslan C.G. 2018: Geology of the Tower Cu-Zn-Ag-Au deposit, sub-Phanerozoic Superior boundary zone, central Manitoba (part of NTS 63G14); Manitoba Growth, Enterprise and Trade, Manitoba Geological Survey, Open File OF2018-4, 38 p.

Couëslan, C.G. 2021: Lithogeochemistry of iron formation, calcsilicate, marble, and mafic dikes from the Thompson nickel belt, central Manitoba (NTS 63O8, 9, 63P5, 12, 15); Manitoba Agriculture and Resource Development, Manitoba Geological Survey, Data Repository Item DRI2021016, Microsoft® Excel® file.

Couëslan, C.G. 2022: Characterization of ultramafic-hosting metasedimentary rocks and implications for nickel exploration at Phillips Lake, Thompson nickel belt, central Manitoba (part of NTS 63O1); Manitoba Natural Resources and Northern Development, Manitoba Geological Survey, Geoscientific Paper GP2022-1, 33 p., 4 appendices.

Couëslan, C.G. 2024: Investigation of volcanic rocks along the eastern margin of the sub-Phanerozoic Thompson nickel belt, central Manitoba (part of NTS 63J3); *in* Report of Activities 2024, Manitoba Economic Development, Investment, Trade and Natural Resources, Manitoba Geological Survey, p. 104–115.

Couëslan, C.G. and Pattison, D.R.M. 2012: Low-pressure regional amphibolite-facies to granulite-facies metamorphism of the Paleoproterozoic Thompson Nickel Belt, Manitoba; Canadian Journal of Earth Sciences, v. 49, p. 1117–1153.

Couëslan, C.G. and Janssens, J. 2025: Whole-rock lithogeochemistry and assays for samples along the eastern margin of the sub-Phanerozoic Thompson nickel belt, central Manitoba (part of NTS 63J3); Manitoba Business, Mining, Trade and Job Creation, Manitoba Geological Survey, Data Repository Item DRI2025012, Microsoft® Excel® file.

Couëslan, C.G., Pattison, D.R.M. and Tinkham, D.K. 2011: Regional low-pressure amphibolite-facies metamorphism at the Pipe II mine, Thompson nickel belt, Manitoba, and comparison of metamorphic isograds in metapelites and meta-iron formations; The Canadian Mineralogist, v. 49, p. 721–747.

de Capitani, C. and Petrakakis, K. 2010: The computation of equilibrium assemblage diagrams with Theriak/Domino software; American Mineralogist, v. 95, no. 7, p. 1006–1016.

Holland, T.J.B. and Powell, R. 1998: An internally-consistent thermodynamic dataset for phases of petrological interest; Journal of Metamorphic Geology, v. 16, no. 3, p. 309–344.

Jensen, L.S. and Pyke, D.R. 1982: Komatiites in the Ontario portion of the Abitibi belt; *in* Komatiites, N.T. Arndt and E.G. Nisbet (ed.), George Allen and Unwin, London, United Kingdom, p. 147–157.

Macek, J.J., Zwanzig, H.V. and Pacey, J.M. 2006: Thompson Nickel Belt geological compilation map, Manitoba (parts of NTS 63G, J, O, P and 64A and B); Manitoba Science, Technology, Energy and Mines, Manitoba Geological Survey, Open File Report, OF2006-33, digital map on CD, URL <https://www.manitoba.ca/iem/info/libmin/OF2006-33.zip> [August 2023].

McDonough, W.F. and Sun, S.-s. 1995: The composition of the Earth; Chemical Geology, v. 120, p. 223–253, URL <https://doi.org/10.1016/0009-2541(94)00140-4>.

Middlemost, E.A.K. 1989: Iron oxidation ratios, norms and the classification of volcanic rocks; Chemical Geology, v. 77, p. 19–26.

Nesbitt, R.W., Sun, S.-s. and Purvis, A.C. 1979: Komatiites: geochemistry and genesis; The Canadian Mineralogist; v. 17, p. 165–186.

Pattison, D.R.M. 1992: Stability of andalusite and sillimanite and the Al_2SiO_5 triple point: constraints from the Ballachulish aureole, Scotland; Journal of Geology, v. 100, p. 423–446.

Pattison, D.R.M. and Tinkham, D.K. 2009: Interplay between equilibrium and kinetics in prograde metamorphism of pelites: an example from the Nelson aureole, British Columbia; Journal of Metamorphic Geology, v. 27, p. 249–279.

Pearce, J.A. 1996: A user's guide to basalt discrimination diagrams; *in* Trace Element Geochemistry of Volcanic Rocks: Applications for Massive Sulphide Exploration, D.A. Wyman (ed.), Geological Association of Canada, Short Course Notes, v. 12, p. 79–113.

Piché, M. and Jébrak, M. 2004: Normative minerals and alteration indices developed for mineral exploration; Journal of Geochemical Exploration, v. 82, p. 59–77.

Simard, R.-L., McGregor, C.R., Rayner, N. and Creaser, R.A. 2010: New geological mapping, geochemical, Sm-Nd isotopic and U-Pb age data for the eastern sub-Phanerozoic Flin Flon Belt, west-central Manitoba (parts of NTS 63J3–6, 11, 12, 14, 63K1–2, 7–10); *in* Report of Activities 2010, Manitoba Innovation, Energy and Mines, Manitoba Geological Survey, p. 69–87, URL <https://www.manitoba.ca/iem/geo/field/roa10pdfs/GS-6.pdf> [July 2025].

Sproule, R.A., Lesher, C.M., Ayer, J.A., Thurston, P.C. and Herzberg, C.T. 2002: Spatial and temporal variations in the geochemistry of komatiites and komatiitic basalts in the Abitibi greenstone belt; Precambrian Research, v. 115, p. 153–186.

Syme, E.C., Lucas, S.B., Bailes, A.H. and Stern, R.A. 1999: Contrasting arc and MORB-like assemblages in the Paleoproterozoic Flin Flon belt, Manitoba, and the role of intra-arc extension in localizing volcanic-hosted massive sulphide deposits; Canadian Journal of Earth Sciences, v. 36, no. 11, p. 1767–1788, URL <https://doi.org/10.1139/e98-084>.

Tinkham, D.K. and Ghent, E.D. 2005: Estimating P-T conditions of garnet growth with isochemical phase diagram sections and the problem of effective bulk-composition; The Canadian Mineralogist, v. 43, p. 35–50.

Tucker, C., Barrie, C.T., Taylor, C. and Ames, D.E. 2005: Geology and metal contents of the Ruttan volcanogenic massive sulfide deposit, northern Manitoba, Canada; Mineralium Deposita, v. 39, p. 795–812.

Waterton, P., Pearson, D.G., Kjarsgaard, B., Hulbert, L., Locock, A., Parman, S. and Davis, B. 2017: Age, origin, and thermal evolution of the ultra-fresh ~1.9 Ga Winnipegosis Komatiites, Manitoba, Canada; Lithos, v. 268–271, p. 114–130.

Winchester, J.A., Park, R.G. and Holland, J.G. 1980: The geochemistry of Lewisian semipelitic schists from the Gairloch district, Wester Ross; Scottish Journal of Geology, v. 16, p. 165–179.

Wood, D.A., Joron, J.-L. and Treul, M. 1979: A re-appraisal of the use of trace elements to classify and discriminate between magma series erupted in different tectonic settings; Earth and Planetary Science Letters, v. 45, p. 326–336.

Zwanzig, H.V. 2005: Geochemistry, Sm-Nd isotope data and age constraints of the Bah Lake assemblage, Thompson Nickel Belt and Kisseynew Domain margin: relation to Thompson-type ultramafic bodies and a tectonic model (NTS 63J, O and P); *in* Report of Activities 2005, Manitoba Industry, Economic Development and Mines, Manitoba Geological Survey, p. 40–53.

Zwanzig, H.V., Macek, J.J. and McGregor, C.R. 2007: Lithostratigraphy and geochemistry of the high-grade metasedimentary rocks in the Thompson Nickel Belt and adjacent Kisseynew Domain, Manitoba: implications for nickel exploration; Economic Geology, v. 102, p. 1197–1216.